HIGHEST FIGURE OF MERIT MICROACOUSTIC RESONATOR FOR MID-BAND 6G APPLICATIONS

Gabriel Giribaldi, Michele Pirro, Meruyert Assylbekova, Luca Colombo, and Matteo Rinaldi
Northeastern SMART Center, Northeastern University, Boston, USA

ABSTRACT

This paper reports on outstanding microacoustic resonators in the 7-11 GHz range of operation, opening the mid-band 6G filtering challenge. By leveraging the superior piezoelectric performance of highly-doped Scandium Aluminum Nitride ($Sc_{0.3}Al_{0.7}N$), Lateral Field Excited (LFE) Cross-sectional Lamé Mode Resonators (CLMRs) were fabricated with a simple (ideally 2-masks) and optimized micro-machining process, attaining record-breaking performance in terms of 3dB quality factor (Q_{3dB}) and single-mode electromechanical coupling (k_{tSM}^2) in that frequency range. Moreover, exploiting CLMRs' lithographic tunability of the resonance frequency, a span of more than 4 GHz in the frequency operation of such devices was achieved on the same chip without complication of the micro-machining process. The fabrication was carried-out on 200 mm wafers, being therefore compatible with industrial grade MEMS foundries. Finally, considerations are drawn in terms of required resonator performance to enable the synthesis of microacoustic filters for the future sixth-generation mobile network.

KEYWORDS

MEMS, CLMR, Sc-doped AlN, RF front-end, 6G, RF filters

INTRODUCTION

The rapid evolution of mobile networks in the last decade has radically changed the way we perceive and interact with the world. Such a technological revolution recently culminated in a first commercial deployment of the fifth-generation cellular wireless (5G), showcasing record-high data-rates [1] and opening windows for the development of the cutting-edge applications of tomorrow. The newly introduced 5G comes with two main frequency bands, the sub-6GHz and the mm-wave one (24-100 GHz). While the first is already highly exploited, the latter has been implemented with limited use cases. Nevertheless, the insatiable demand for technology to furtherly pervade our lives is already pushing research toward the 6G era. In that framework, new frequency bands will be allocated, going from the sub-GHz devoted to extreme wide area Internet of Things and rural areas coverage to the sub-THz for ultra-short-range communication with maximized data-rate [2]. According to [2], the frequency spectrum allocated to urban areas will be the 7-20 GHz band, providing an excellent trade-off between network capacity and coverage.

Although the bright premises, the practical implementation of such a 6G capacity revolution requires radically new technologies. In particular, heavy innovation in the radio frequency front-ends (RFFE) will be indispensable to allow for the 6G to become a reality.

The focus of the present work is on the filtering elements, RFFE blocks with the fundamental task of removing any undesired frequency component which may corrupt the carrier signal. In particular, the expected transition from the 100 MHz component carrier bandwidth of 5G to the 400 MHz of 6G [2] will require tremendous improvements in the performance of the microacustic filters. This directly translates into more and more stringent requirements for the Microelectromechanical (MEM) resonators used as their building blocks. Specifically, the devices will need higher operating frequencies (f_s>*7* GHz) in order to work in the new bands, high electromechanical coupling ($k_t^2>4\%$) in order to allow for a bandwidth of >400 MHz and relatively high quality factors ($Q>250$) to ensure low loss and proper filter selectivity. Those specifications result in the unprecedented requirement of a technological Figure of Merit (FoM) $f_s \cdot Q \cdot k_t^2>100GHz$.

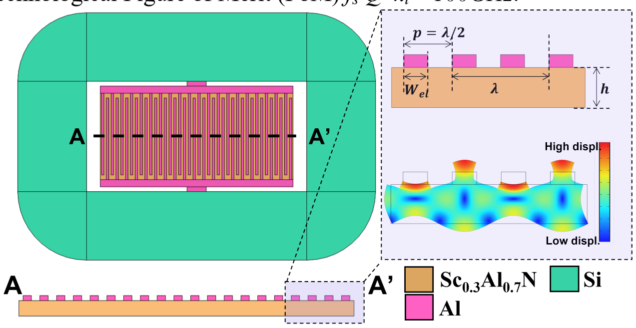

Figure 1: 3D and 2D view of a CLMR from this work, with highlighted relevant dimensions. In particular, the horizontal acoustic wavelength (λ), the pitch (p), the electrode width (W_{el}), and the piezoelectric thickness (h). Moreover, the CLMR mode-shape, obtained via COMSOL Multiphysics Finite Element Modeling simulation is given.

The current state-of-the art in terms of microacoustic resonators is constituted by thin-Film Bulk Acoustic Resonators (FBARs), developed in the '90s [3]. Since their commercialization, an incredible amount of research has been conducted to solve FBARs' limitations related to lithographic frequency tunability and scaling >5 GHz [4][5][6]. Nevertheless, the lower performance or higher fabrication complexity of alternative solutions have relegated them to the research realm, leaving FBARs as the only market player. Only recently the Cross-sectional Lamé Mode Resonator (CLMR) technology has been proposed [7] (Fig.1), attaining performance comparable to FBARs, but also achieving lithographic frequency tunability and offering unprecedented scaling capabilities with demonstrated f_s of 11 GHz [8] and 23 GHz [9] (overtone) with Q>*600* and *250*, respectively, employing a single interdigital electrode configuration. Nevertheless, due to the relatively low piezoelectric coupling achievable with such electrodes on AlN (k_t^2<2%), those devices did not meet the bandwidth requirements of the emerging mid-band 6G spectrum. Doping of AlN with large concentrations of Sc (>20%) has been recently demonstrated as an effective solution to achieve a 3-to-5-fold k_t^2 improvement in CLMRs [10][11]. Nevertheless, such a k_t^2 increase has been so far attained at the cost of a reduced $f_s \cdot Q$ product FoM, particularly for Sc concentrations ≥20\% due to limitations in material quality, resonator design, and/or micro-machining process [12][13].
This paper presents therefore the first technological solution for the mid-band 6G filtering challenge. In particular, we experimentally demonstrate microacoustic resonators operating in the 7-11 GHz range with record-breaking FoM, and we show devices with $f_s \cdot Q \cdot k_t^2>140$ GHz. Differently from the state-of-the-art in the same frequency range [12][13][14], we not only achieve a ~4X k_t^2-boost through high Sc-doping but we also demonstrate that high $f_s \cdot Q$ products, comparable to the one of the more mature AlN, can be achieved in highly-doped ScAlN resonators, which provides an

answer to the most important outstanding question in this research field. Finally, we draw considerations about the possible commercialization and mass production of such devices, also thanks to the very easy fabrication process carried out on MEMS-foundry standard 200 mm wafers, ScAlN post-CMOS compatibility, and the very good agreement of experimental results and finite element modeling (FEM) simulations.

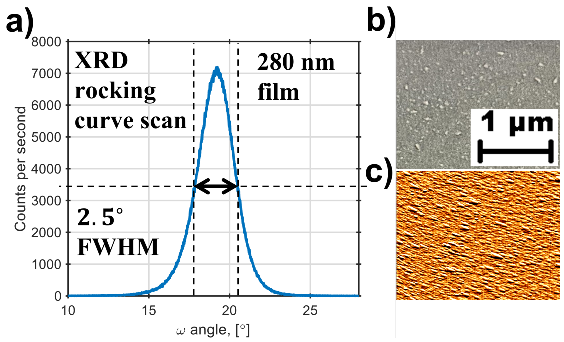

Figure 2: a) X-Ray Diffractometry (XRD) Rocking Curve scan of the 280 nm ScAlN film employed in this work. (b) and (c) show Scanning Electron Microscope (SEM) and Atomic Force Microscope (AFM) top views of the film's surface, respectively.

FABRICATION

Highly c-axis oriented ScAlN films

A 280 nm $Sc_{0.3}Al_{0.7}N$ thin-film was deposited on a high-resistivity 200 mm Si<100> wafer via reactive sputtering utilizing an industrial grade EVATEC Clusterline II tool. A 12" compound $Al_{0.7}Sc_{0.3}$ casted target was employed as source. A thorough optimization process was followed in order to obtain the high film quality. In particular, the metrics of interest were: the Full Width Half Maximum (FWHM, Fig.2a, with a measured value of 2.5°), the in-plane stress and stress gradient, the surface roughness, and the Abnormally Oriented Grains (AOGs) count (Fig.2b-c). Moreover, the sputtering process could count on a high throughput (47 nm/min). The recipe utilized a Nitrogen flow of 90 sccm, a power of 6 kW applied to the AlSc target, a chuck-height of 20 mm, and a temperature to 300°C.

Microacoustic resonators

After the film was deposited, the etch of the piezoelectric layer took place in order to define the resonant plates. The process took advantage of an optimized dry etching recipe performed in an Oxford Inductively Coupled Plasma (ICP) Reactive Ion Etching (RIE) tool, in conjunction with an oxide mask deposited via Plasma Enhanced Chemical Vapor Deposition (PECVD) and etched in fluorine chemistry. The ScAlN etching recipe utilized chlorine chemistry and high argon flow, with 10 sccm of Cl_2, 6 sccm of BCl_3, and 28 sccm of Ar. High power levels were utilized, with 300 W RF and 600 W ICP power. The etching pressure was 10 mTorr. After the etch of the piezo-layer, the oxide mask was stripped in 49% hydrofluoric acid (HF). The combination of an optimized etching recipe and a hard mask resulted in straight sidewalls (>70°).
Subsequently, the nanometric finger electrodes (W_{el}=*140-300 nm*) were defined via electron beam lithography and Aluminum thermal evaporation. In terms of photoresist, the e-beam step employed a bi-layer of PMGI SF3 (lift-off resist) and PMMA A7. The lift-off itself was performed in Microposit Remover 1165 heated at 85°C. In order to ease the very low throughput e-beam step, only the finger electrodes were defined, while the routing was fabricated in a second moment utilizing a direct writer and Aluminum sputtering and lift-off. In the scenario of a possible mass production of such devices, the e-beam and direct writer litho steps could be combined with the aid of a deep-UV stepper. Finally, the devices were released via XeF_2 isotropic etching (Fig.3 for a view of the fabrication steps and SEMs of fabricated devices).

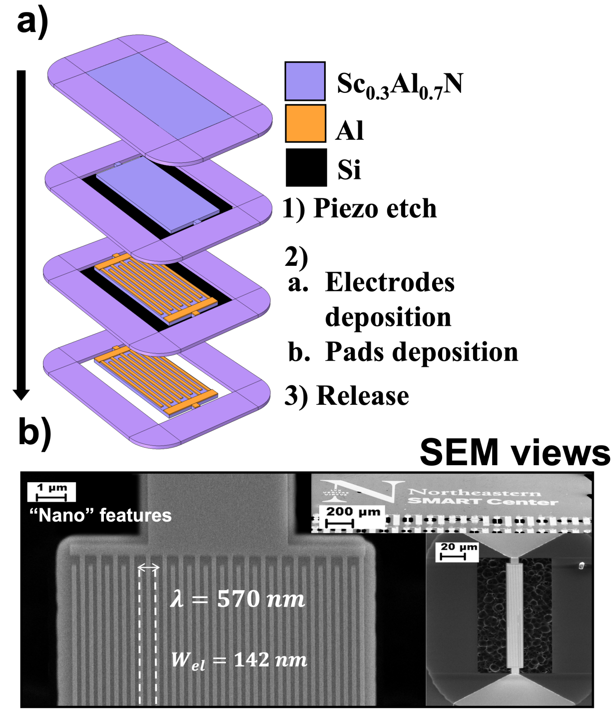

Figure 3: a) Employed micro-machining process and b) SEM pictures of devices presented in this work.

EXPERIMENTAL RESULTS

The device testing was carried out through direct probing with two Cascade GSG150 RF probes. The devices scattering parameters were recorded utilizing a Keysight N5221A network analyzer.
The fabricated resonators exhibited resonances in the 7-11 GHz range, therefore demonstrating a wide on-chip tunability of the operating frequency without major k_t^2 degradation. The admittance responses (Y_{12} vs. frequency) of outstanding devices are reported in Fig.4a, along with relevant metrics and FoM. Moreover, Fig.4b shows a comparison of the admittance response of a resonator of this work with the AlN-based one of [8], working at the same frequency. By employing COMSOL® Multiphysics, the same devices were *a-posteriori* FEM-simulated. In this way, the simulations could count on the actual measured geometrical dimensions. A mechanical quality factor equal to the 3dB one of the measured resonators was superimposed. In order to simulate ScAlN, not present in the COMSOL library, a custom material utilizing the ab-initio equations derived in [10] for the piezoelectric and mechanical properties was employed. As dielectric constant, instead, an experimentally extracted value of 17 was used. It was measured with an aixACCT TF2000 thin-film characterization tool with a procedure similar to the one of [15]. The simulation admittance results are shown in Fig.4a. Moreover, Fig.4c-d reports a comparison of the measured resonance frequency and electromechanical coupling between the experimental measurements and the simulations, as function of the geometrical ratio of the piezoelectric thickness and the horizontal acoustic wavelength (h/λ). Each single datapoint is the result of a set of 3 measurements on similar devices. As it can be observed, the f_s value can be predicted with a high degree of accuracy, with a maximum relative error of about 2%. In terms of k_t^2, it can be

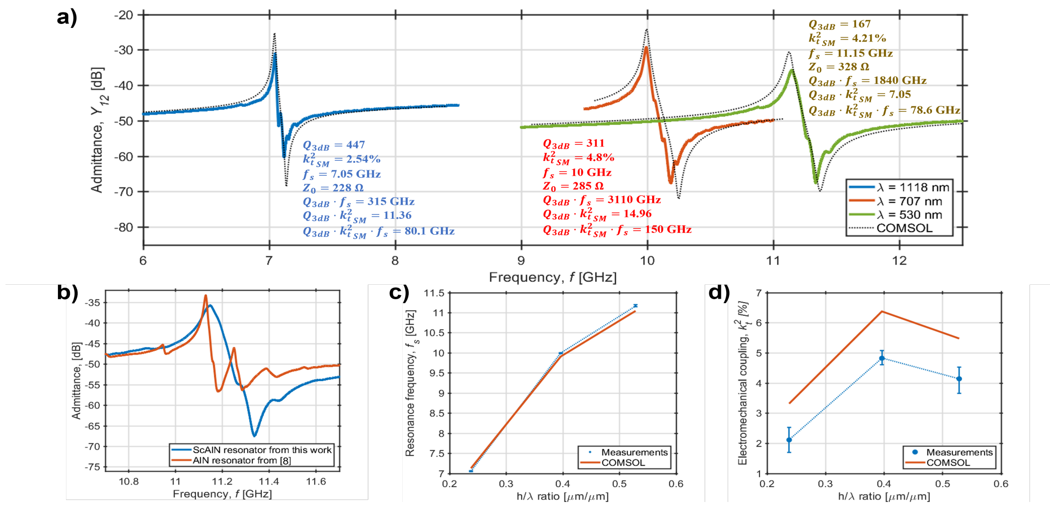

Figure 4: a) Admittance Y_{12} plots vs. frequency of three showcase resonators of this work, with highlighted main metrics and FoM. In b), a ScAlN resonator of this work is compared to a similar design in AlN from [8], showing the 3.3-fold k_t^2 improvement. In c) and d), the experimental results are compared to a-posteriori COMSOL simulations in terms of resonance frequency and k_t^2, respectively. Each datapoint is the result of the average on 3 similar devices, and the extreme cases are shown in the error bars.

observed that the trend of the measurements matches the one of the simulations, with maximum coupling for $h/\lambda = 0.4$ as in [11]. Nevertheless, there is an offset between the two curves. This is because (i) all the material properties in COMSOL besides the dielectric constant come from *ab-initio* calculations and do not necessarily reflect the real values and (ii) the simulations do not take into account material non-idealities, such as a FWHM of 2.5° and some (even if few) AOGs on the top surface. Further optimization in the thin-film deposition parameters has to be performed in order to reduce the gap between measurements and simulations.

IMPACT

The unprecedented performance of the aforementioned devices opens wide possibilities in the world of RF-MEMS. In fact, it firstly sparkles new interest in the CLMR technology, now seen as a possible solid alternative to FBARs in the framework of commercial filtering devices above 5 GHz. Moreover, the obtained resonator quality factors, especially in such a frequency range, prove that recurring to high Sc-doping of AlN, though boosting the electromechanical coupling through an enhancement of the piezoelectric coefficients, does not necessarily translate in a Q degradation as stated in [16]. Furthermore, the demonstrated wide on chip tunability of the resonance frequency obtained simply by lithographically adjusting the horizontal acoustic wavelength allows, in that frequency range, to sweep the device operation of several GHz without major deterioration of the k_t^2. This provides a substantial improvement in design flexibility compared to FBARs and allows to cover multiple bands with filters fabricated on the same substrate without overcomplications of the micro-machining process, thus providing cost-effectiveness. Finally, the present devices represent the first attempt to solve the mid-band 6G filtering challenge. The scatter plots of Fig.5 show a comparison of the devices of this work with similar designs (AlN and ScAlN CLMRs) present in the literature, showcasing the undisputed performance superiority in terms of relevant FoM, as a result of all-around design and fabrication optimizations. Moreover, in the same plots the optimal region of operation of MEMS resonators allowing the synthesis of microacoustic filters for the 6G mid-band is highlighted.

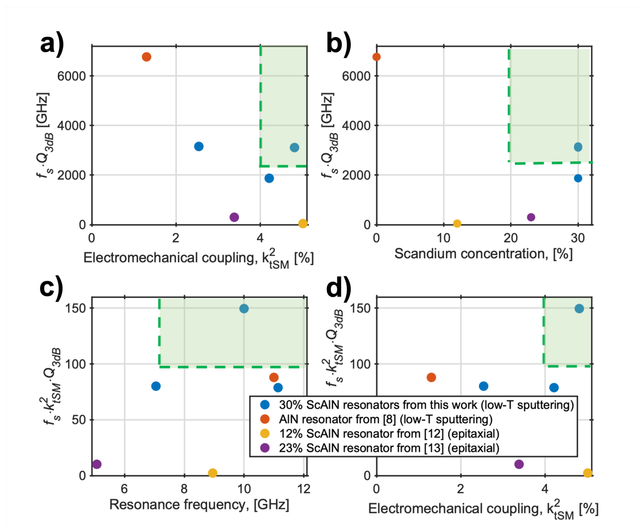

Figure 5: Scatter plots comparing the performance of the resonators in Fig.4a to the ones of [8] (with a sputtered piezoelectric layer) and [12][13] (with an epitaxial piezoelectric layer, therefore not CMOS-compatible). The metrics are the 3dB quality factor (Q_{3dB}) and the single-mode electromechanical coupling (k_{tSM}^2). The optimal performance region for the synthesis of high-performance filters for the mid-band 6G spectrum is highlighted.

CONCLUSIONS

The present work introduced and opened the 6G mid-band filtering challenge, with the final aim of enabling the filtering hardware required for the next-generation mobile network in urban areas. In particular, the focus was on highly-doped ScAlN and CLMR technology for the piezo-material and the design counterparts, respectively. Their combination is foreseen by the authors to allow for the synthesis of high-performance, compact and cost-effective microacoustic filters and duplexers for the RF front-ends of future commercial mobile devices.

Outstanding microacoustic resonators in the 7-11 GHz range of operation have been presented, with the most performing one featuring $Q_{3dB} \cdot k_{tSM}^2 \cdot f_s > 140\,GHz$, along with accurate post-fabrication Finite Element Modeling simulation results. Such an accomplishment is the result of an all-around optimization process targeting high-quality and highly-doped ScAlN thin films on 200 mm substrates, most-performing designs, and minimization of fabrication-related design non-idealities, e.g. resonator plate sidewalls, layer to layer misalignment, and finger coverage.

Finally, devices from this work have been compared with similar designs with resonance frequency above 5 GHz, showing a significant degree of improvement in the most relevant figures of merit.

ACKNOWLEDGEMENTS

This work was supported by Raytheon Missiles and Defense under contract No. 4202341711. The author also wants to thank the staff of the Kostas Nano and Microfabrication Research Center at Northeastern University and the one of the Center for Nanoscale Systems at Harvard University.

REFERENCES

[1] "IEEE 5G and beyond technology roadmap white paper," 2017.

[2] H. Holma, H. Viswanathan, and P. Mogenses, "Extreme massive MIMO for macro cell capacity boost in 5G-advanced and 6G," in Nokia Bell Labs, White paper, 2021.

[3] R. C. Ruby and P. P. Merchant, "Tunable thin film acoustic resonators and method for making the same," in US Patent US5587620A, 1996.

[4] M. Rinaldi, C. Zuniga, and G. Piazza, "5-10 GHz AlN contour-mode nanoelectromechanical resonators," in 2009 IEEE 22nd International Conference on Micro Electro Mechanical Systems, pp. 916–919, 2009.

[5] M. Rinaldi, C. Zuniga, C. Zuo, and G. Piazza, "Super-high-frequency two-port AlN contour-mode resonators for RF applications," IEEE Transactions on Ultrasonics, Ferroelectrics, and Frequency Control, vol. 57, no. 1, pp. 38–45, 2010.

[6] S. Gong and G. Piazza, "Design and analysis of lithium–niobate-based high electromechanical coupling RF-MEMS resonators for wideband filtering," IEEE Transactions on Microwave Theory and Techniques, vol. 61, no. 1, pp. 403–414, 2013.

[7] C. Cassella, Y. Hui, Z. Qian, G. Hummel and M. Rinaldi, "Aluminum Nitride Cross-Sectional Lamé Mode Resonators," in Journal of Microelectromechanical Systems, vol. 25, pp. 275–285, April 2016.

[8] M. Assylbekova, G. Chen, G. Michetti, M. Pirro, L. Colombo, and M. Rinaldi, "11 GHz lateral-field-excited aluminum nitride cross-sectional Lamé mode resonator," in 2020 Joint Conference of the IEEE International Frequency Control Symposium and International Symposium on Applications of Ferroelectrics (IFCS-ISAF), pp. 1–4, 2020.

[9] M. Assylbekova, G. Chen, M. Pirro, G. Michetti, and M. Rinaldi, "Aluminum nitride combined overtone resonator for millimeter wave 5G applications," in 2021 IEEE 34th International Conference on Micro Electro Mechanical Systems (MEMS), pp. 202–205, 2021.

[10] M. A. Caro, S. Zhang, T. Riekkinen, M. Ylilammi, M. A. Moram, O. Lopez-Acevedo, J. Molarius, and T. Laurila, "Piezoelectric coefficients and spontaneous polarization of ScAlN," in Journal of Physics: Condensed Matter, vol. 27, May 2015.

[11] G. Giribaldi, L. Colombo, B. Fabio, C. Cassella, and M. Rinaldi, "Investigation on the impact of scandium-doping on the k_t^2 of $Sc_xAl_{1-x}N$ cross-sectional Lame' mode resonators," IEEE International Ultrasonics Symposium 2020, 2020.

[12] M. Park, Z. Hao, R. Dargis, A. Clark, and A. Ansari, "Epitaxial aluminum scandium nitride super high frequency acoustic resonators," Journal of Microelectromechanical Systems, vol. 29, no. 4, pp. 490–498, 2020.

[13] M. Park and A. Ansari, "Epitaxial $Al_{0.77}Sc_{0.23}N$ SAW and lamb wave resonators," in 2020 Joint Conference of the IEEE International Frequency Control Symposium and International Symposium on Applications of Ferroelectrics (IFCS-ISAF), pp. 1–3, 2020.

[14] M. Park, Z. Hao, D. G. Kim, A. Clark, R. Dargis, and A. Ansari, "A 10 GHz single-crystalline scandium-doped aluminum nitride Lamb-wave resonator," in 2019 20th International Conference on Solid-State Sensors, Actuators and Microsystems Eurosensors XXXIII (TRANSDUCERS EUROSENSORS XXXIII), pp. 450–453, 2019.

[15] M. Pirro, B. Herrera, M. Assylbekova, G. Giribaldi, L. Colombo, and M. Rinaldi, "Characterization of dielectric and piezoelectric properties of ferroelectric AlScN thin films," in 2021 IEEE 34th International Conference on Micro Electro Mechanical Systems (MEMS), pp. 646–649, 2021.

[16] R. H. Olsson, Z. Tang, and M. D'Agati, "Doping of aluminum nitride and the impact on thin film piezoelectric and ferroelectric device performance," in 2020 IEEE Custom Integrated Circuits Conference (CICC), pp. 1–6, 2020.

CONTACT

Gabriel Giribaldi, giribaldi.g@northeastern.edu